Intelligence & Control
https://www.sciltp.com/journals/ic

Article

Fixed-Time Synchronization of Spatiotemporal Networks via Quantized Boundary Control

Tingting Shi [1], Cheng Hu [1,2,*] and Juan Yu [1,2]

[1] College of Mathematics and System Science, Xinjiang University, Urumqi 830017, China
[2] Xinjiang Key Laboratory of Applied Mathematics (XJDX1401), Urumqi 830017, China
* Correspondence: hucheng@xju.edu.cn

How To Cite: Shi, T.; Hu, C.; Yu, J. Fixed-Time Synchronization of Spatiotemporal Networks via Quantized Boundary Control. *Intelligence & Control* **2025**, *1*(1), 3.

Received: 20 May 2025
Revised: 24 July 2025
Accepted: 15 August 2025
Published: 3 September 2025

Abstract: In this paper, the fixed-time synchronization of spatiotemporal networks under quantized boundary control is investigated, where the network coupling encompasses both state coupling and spatial diffusion coupling. First, under the mixed boundary condition, two innovative power-law controllers embedded with a quantization mechanism are designed, and the controllers operate at the boundary of the spatial domain. Subsequently, by employing inequality techniques and fixed-time stability theory, several verifiable criteria are derived to ensure the fixed-time synchronization of the addressed spatiotemporal networks. Lastly, the theoretical results are validated through by numerical simulations of two illustrative examples.

Keywords: spatiotemporal network; fixed-time synchronization; quantized boundary control; spatial diffusion coupling

1. Introduction

Spatiotemporal complex networks (STCNs) are dynamic network models that integrate both temporal and spatial dimensions. They can accurately characterize complex diffusion phenomena, such as the spread of invasive species in ecological populations [1] and the concentration changes of the substances during chemical reactions [2]. Spatial diffusion is a key feature of numerous complex systems. For instance, multilayered cellular neural networks comprise interconnected computing units, where local intercellular interactions represent reaction components, and the information flow among cells corresponds to diffusion components [3]. This example demonstrates that the structure and dynamic behavior of multilayered cellular neural networks depend not only on temporal evolution and spatial position of each cell but also on the information interactions dictated by the spatial distribution of the entire network. Therefore, it is reasonable and significant to consider STCNs.

Synchronization is a common phenomenon in both nature and technology, as seen in the synchronized swinging of coupled pendulums and the synchronized flashing of fireflies. In addition, synchronization plays a crucial role in modern technology, particularly in telecommunications, where devices must align their signals to ensure clear and efficient communication. These examples underscore the importance and ubiquity of synchronization in both natural and artificial systems. Recently, there has been an increasing focus on the study of STCNs [4–6] and various control schemes addressing their synchronization issues, such as impulsive pinning control [7], event-triggered control [8,9], and intermittent control [10]. These traditional control schemes require actuators to be uniformly distributed throughout the entire spatial domain, which poses significant engineering challenges. For instance, consider the intelligent traffic control of urban road systems. If a signal light control system is implemented across an entire road section, it not only entails a substantial investment in installing signal lights and communication networks along hundreds of roads but also faces practical challenges such as high maintenance costs and unreliable power supply in remote areas [11]. To address these challenges, boundary control has been introduced, regulating only the actuators at the boundary of the spatial domain to achieve the desired performance. Currently, boundary control has emerged as a classic control method for studying the synchronization of STCNs and is widely used in the canalization of irrigation networks [12] and flexible riser systems [13].

Recently, the synchronization of STCNs through boundary control has garnered significant research interest. For instance, a backstepping-based boundary controller was devised to ensure synchronization of coupled partial differential systems with Dirichlet boundary conditions [14]. Utilizing the Lyapunov method, state-feedback boundary controllers were designed to achieve exponential and asymptotical synchronization of coupled STCNs with Neumann boundary conditions, respectively [15,16]. Notably, Yang et al. developed a collocated boundary control scheme that employs boundary measurement for cluster synchronization of STCNs, wherein the controller only relies on spatial boundary states [17]. Additionally, researchers have integrated different advanced control strategies with boundary control to address STCN synchronization, including adaptive control [18], pinning control [19], and quantized control [20,21]. Among these effective control schemes, quantized control is particularly advantageous in scenarios with limited communication capacity or constrained processing power. Examples include bandwidth-constrained large-scale smart grids and long-distance data transmission for a pipeline boundary sensor. By converting continuous control inputs into discrete values characterized by limited precision, quantized control reduces data transmission and mitigates channel congestion. Recently, this approach has found widespread application in digital control systems, digital signal processing, and computer-based control systems [22]. Xiong et al. successfully addressed the drive-response synchronization of stochastic systems by incorporating a quantitative mechanism into the intermittent control scheme [23]. Interestingly, Yang et al. introduced a novel and cost-effective quantized communication mechanism in their modeling, providing a practical solution to the challenges posed by limited communication bandwidth [24]. However, the models in these studies focused solely on state coupling. In reality, spatial diffusion coupling often exists in many practical networks, as individual diffusion processes can mutually affect neighboring individuals. A typical example is predator-prey systems, where invasive species may lead to population flux variations [1]. In recent years, limited progress has been made in addressing synchronization of STCNs with spatial diffusion coupling [10,25]. However, the quantized boundary synchronization of STCNs with spatial diffusion coupling remains an open problem.

It is noteworthy that existing results mainly focused on asymptotic or exponential synchronization of STCNs as time approaches infinity. Nonetheless, such infinite-time convergence can be impractical for real-world applications due to the lifespan limitation of biologies and devices. To expedite the convergence of the controlled system, the concept of finite-time synchronization was put forward [26]. Motivated by its superior anti-interference capability and enhanced robustness, the finite-time synchronization of STCNs has been thoroughly studied [27,28]. Luo et al. examined the finite-time synchronization of STCNs through boundary control based on Lyapunov stability theory in [29]. Notably, in [30,31], the finite-time stabilization of reaction-diffusion systems, both with and without delay, was investigated using boundary control methods. It should be noted that the settling time in these synchronization results critically relies on the initial states of the target system, which are often unavailable a priori. Consequently, Polyakov introduced the concept of fixed-time stability in [32], where the convergence time depends on the system parameters and control parameters. Following this, numerous excellent fixed-time stability results have been published, contributing to the study of fixed-time synchronization in complex systems [33–35].

Currently, advancements in fixed-time synchronization of STCNs have gradually matured, with fixed-time theoretical frameworks established for various network models, including neural networks with time-varying coefficients and time delay [36], complex-valued neural networks [37], Hopfield neural networks with delays [38], and complex-valued memristive neural networks with Markovian jump parameters [39]. However, these results focused on full-domain controllers distributed throughout the entire space, often resulting in high costs and technical challenges during engineering implementation. In contrast to those control designs with full-domain measurements, Espitia et al. devised a time-varying boundary controller distributed on the Dirichlet boundary and established fixed-time stabilization conditions of STCNs based on the backstepping approach [40]. Li et al. developed two piecewise feedback controllers distributed on the Neumann boundary and mixed boundary based on the quadratic norm in the Sobolev space, allowing the states of STCNs to achieve synchronization within a fixed time [41]. In [42], a logarithmic quantization mechanism was incorporated into the boundary controller for STCNs to ensure fixed-time synchronization. Notably, the boundary controllers proposed in [41,42] consist of a linear feedback part and power-law terms, which are tedious and laborious. Additionally, these studies also overlook the crucial role of spatial diffusion coupling. Thus, optimizing these control schemes to achieve fixed-time synchronization of STCNs with spatial diffusion coupling via quantized boundary control is a central problem that needs to be addressed.

Inspired by the aforementioned analysis, this article investigates the fixed-time synchronization of STCNs with hybrid coupling via quantized boundary control. The primary novelties of this article are summarized below.

(1) To capture the intricate dynamics of network interactions, a class of STCNs integrating state coupling and spatial diffusion coupling is considered, which enhances the generalization capability of the single-coupling models proposed in [29–31,36–40].

(2) To achieve fixed-time synchronization of STCNs with or without spatial diffusion coupling, two types of quantized boundary controllers without a linear feedback term are devised. Compared to the full-domain controllers presented in [7,8,10], the boundary control strategies designed here are more cost-effective and easier to implement. Specifically, the proposed boundary controllers incorporate a quantization mechanism, reducing the communication burden and computational overhead compared to existing boundary control schemes [29,30].

(3) By directly constructing Lyapunov functions, several sufficient conditions are put forward to ensure fixed-time synchronization of STCNs with mixed boundary conditions. Distinguished from previous studies [15–19,29] that mainly focused on Neumann boundary conditions, our theoretical analysis eliminates complicated variable transformation, significantly simplifying the mathematical derivation process.

The remainder of this paper is arranged as follows. Section 2 introduces some necessary preliminaries. In Section 3, the fixed-time synchronization of STCNs is investigated under quantized boundary control. In Section 4, two simulated examples are presented to validate the feasibility of the derived results. Finally, Section 5 concludes this article.

Notations. The set of all real numbers is denoted by R. $\mathcal{R}^n$ and $\mathcal{R}^{n\times m}$ represent the spaces of all n-dimensional real vectors and $n \times m$-dimensional real matrices, respectively. $\mathcal{N} = \{1, 2, \ldots, m\}$, where m is a positive integer. For any $y \in \mathcal{R}^n$, $\|y\| = \sqrt{y^T y}$, where y^T represents its transpose, $|y| = (|y^1|, |y^2|, \ldots, |y^n|)^T$, $\text{sign}(y) = (\text{sign}(y^1), \text{sign}(y^2), \ldots, \text{sign}(y^n))^T$. For any symmetric matrix $P \in \mathcal{R}^{n\times n}$, $\lambda_{\max}(P)$ and $\lambda_{\min}(P)$ denote the maximum eigenvalue and the minimum eigenvalue of P, respectively. The matrix norm is denoted by $\|P\| = \sqrt{\lambda_{\max}(P^T P)}$. P^{-1} represents the inverse of a nonsingular P. I_n is an n-order identity matrix. $\mathbf{0}_m \in \mathcal{R}^m$ is a column vector where all elements are 0. $[P]^s = P + P^T$. For a real matrix P, the notation $P > 0$ indicates that the matrix P is positive-definite. diag$\{\cdot\}$ denotes a diagonal matrix, and $\otimes$ represents the Kronecker product. For any $z(\nu, t) = (z^1(\nu, t), z^2(\nu, t), \ldots, z^n(\nu, t))^T : [0, L] \times [0, +\infty) \mapsto \mathcal{R}^n$, denote $\|z(\cdot, t)\|_{\mathcal{L}_2} = \left(\int_0^L \sum_{r=1}^{n} (z^r(\nu, t))^2 \mathrm{d}x \right)^{\frac{1}{2}}$.

2. Model Description and Preliminaries

Consider a spatiotemporal network with spatial diffusion coupling and state coupling, where the state of each vertex is described by the following

$$\begin{aligned} \frac{\partial z_r(x,t)}{\partial t} =& D\Delta z_r(x,t) + Az_r(x,t) + Bf(z_r(x,t)) \\ &+ \varepsilon \sum_{j=1}^{m} w_{rj} \Gamma \Delta z_j(x,t) + \varepsilon \sum_{j=1}^{m} w_{rj} \hat{\Gamma} z_j(x,t), \end{aligned} \tag{1}$$

where $r \in \mathcal{N}$, $z_r(x,t) = (z_r^1(x,t), z_r^2(x,t), \ldots, z_r^n(x,t))^T$, $(x,t) \in (0, L) \times (0, +\infty)$ is the spatio-temporal state of the rth vertex, $\Delta = \frac{\partial^2}{\partial x^2}$ denotes the Laplace diffusion operator, $f(z_r(x,t)) \in \mathcal{R}^n$ is a continuous nonlinear vector function, $D = \text{diag}\{d_1, d_2, \ldots, d_n\} > 0$ represents a transmission diffusion coefficient matrix, A and B are n-order matrices, $\varepsilon > 0$ stands for the overall coupling strength, $\Gamma = \text{diag}\{\gamma_1, \gamma_2, \ldots, \gamma_n\}$ and $\hat{\Gamma} = \text{diag}\{\hat{\gamma}_1, \hat{\gamma}_2, \ldots, \hat{\gamma}_n\}$ are positive-definite inner coupling matrices, matrix $W = (w_{rj})_{m\times m}$ depicts the network topology, where $w_{rj} = w_{jr} \neq 0$ if there is communication between vertex r and vertex j; otherwise, $w_{rj} = 0$ $(r \neq j)$, and $w_{rr} = -\sum_{j=1, r\neq j}^{m} w_{rj}$. Here, it is assumed that the network topology corresponding to the coupling matrix W is undirected, without self-loops and without any connectivity restrictions.

Remark 1. *Most existing studies on fixed-time synchronization of STCNs have mainly focused on state coupling, while spatial diffusion coupling has garnered relatively limited attention [36–39]. Nonetheless, in real-world scenarios, the heterogeneous spatial diffusion of individual nodes can have a great impact on the dynamics of other nodes within the network. Therefore, it is crucial to incorporate spatial diffusion coupling into the analysis of STCNs.*

The initial value and the mixed boundary conditions of system (1), which consists of Dirichlet and Neumann boundary conditions, are given by

$$\begin{cases} z_r(x,0) = z_r^0(x), \quad x \in (0, L], \\ z_r(0,t) = \mathbf{0}_n, \quad \left.\dfrac{\partial z_r(x,t)}{\partial x}\right|_{x=L} = U_r(t), \quad t \in [0, +\infty) \end{cases}$$

where $r \in \mathcal{N}$, $U_r(t) = (U_r^1(t), U_r^2(t), \ldots, U_r^n(t))^T$ is a boundary control input.

The desired synchronization state is denoted as $\xi(x,t) \in R^n$ *and satisfies*

$$\begin{cases} \dfrac{\partial \xi(x,t)}{\partial t} = D\Delta\xi(x,t) + A\xi(x,t) + Bf(\xi(x,t)), \ \ (x,t) \in (0,L) \times (0,+\infty), \\ \xi(x,0) = \xi^0(x), \ \ x \in (0,L], \\ \xi(0,t) = \dfrac{\partial \xi(x,t)}{\partial x}\Big|_{x=L} = \mathbf{0}_n, \ \ t \in [0,+\infty). \end{cases} \tag{2}$$

Define the synchronization error $\sigma_r(x,t) = (\sigma_r^1(x,t), \ldots, \sigma_r^n(x,t))^T = z_r(x,t) - \xi(x,t)$. *In the following, the synchronization error system can be obtained by subtracting (1) from (2),*

$$\begin{cases} \dfrac{\partial \sigma(x,t)}{\partial t} = (I_m \otimes D)\Delta\sigma(x,t) + (I_m \otimes A)\sigma(x,t) + (I_m \otimes B)F(\sigma(x,t)) \\ \qquad\qquad + \varepsilon(W \otimes \Gamma)\Delta\sigma(x,t) + \varepsilon(W \otimes \hat{\Gamma})\sigma(x,t), \ \ x \in (0,L), \\ \sigma^0(x) = z^0(x) - \xi^0(x), \ \ x \in (0,L], \\ \sigma(0,t) = \mathbf{0}_{nm}, \ \ \dfrac{\partial \sigma(x,t)}{\partial x}\Big|_{x=L} = U(t), \ \ t \in [0,+\infty), \end{cases} \tag{3}$$

where $\sigma(x,t) = (\sigma_1^T(x,t), \ldots, \sigma_m^T(x,t))^T$, $F(\sigma(x,t)) = (\tilde{f}^T(\sigma_1(x,t)), \ldots, \tilde{f}^T(\sigma_m(x,t)))^T \in \mathcal{R}^{nm}$, $\tilde{f}(\sigma_r(x,t)) = f(z_r(x,t)) - f(\xi(x,t)) \in \mathcal{R}^n$, $r \in \mathcal{N}$, $U(t) = (U_1^T(t), U_2^T(t), \ldots, U_m^T(t))^T \in \mathcal{R}^{nm}$.

Definition 1 ([39]). *The network (1) with boundary control* $U(t)$ *is called fixed-time synchronized if there exist a fixed time* $T_{\max} \geq 0$ *and a settling time function* $T(\sigma^0(\cdot)) \geq 0$ *satisfying* $T(\sigma^0(\cdot)) \leq T_{\max}$ *such that*

$$\begin{cases} \lim\limits_{t \to T(\sigma^0(\cdot))} \|\sigma(\cdot,t)\|_{\mathcal{L}_2} = 0, \\ \sigma(x,t) = \mathbf{0}_{nm}, \ \ x \in [0,L], \ \ t \geq T(\sigma^0(\cdot)). \end{cases}$$

Remark 2. *Based on the error system (3), the synchronization control problem of the STCN (1) is converted to the stabilization of the error system (3). Fixed-time synchronization implies that all states* $z(x,t)$*, whether at the boundary or within the spatial domain, can converge to the synchronization state* $\xi(x,t)$ *within the fixed time* $T_{\max}$*. In [36–39], the definition of fixed-time synchronization under Dirichlet boundary conditions is provided, where* $\sigma(x,t) = \mathbf{0}_{nm}$ *is required just for* $t \geq T_{\max}$ *and* $x \in (0,L)$ *since* $\sigma(L,t) = \mathbf{0}_{nm}$ *and* $\sigma(0,t) = \mathbf{0}_{nm}$ *are naturally satisfied for* $t \geq 0$*. Nonetheless, the natural result may not be true in spatiotemporal networks with mixed boundary conditions. Consequently, a stricter spatial domain restriction* $x \in [0,L]$ *is established for* $\sigma(x,t) = \mathbf{0}_{nm}$ *in Definition 1.*

The primary objective of our study is to design a boundary feedback controller $U_r(t)$ *that ensures synchronization of the coupled network (1) within a fixed time. To derive the main results, some necessary assumptions and relevant lemmas are given below.*

Lemma 1 ([16]). *Suppose that* $F(r) : [0,L] \to \mathcal{R}^n$ *is a continuous and square integrable function satisfying* $F(0) = 0$ *or* $F(L) = 0$*. Then, for a matrix* $Q > 0$*,*

$$\int_0^L F^T(r)QF(r)dr \leq \frac{4L^2}{\pi^2}\int_0^L \Big(\frac{dF(r)}{dr}\Big)^T Q\Big(\frac{dF(r)}{dr}\Big)dr.$$

Lemma 2 ([34]). *If there exists a positive-definite and radially unbounded function* $F(x(t)) : R^n \mapsto R$ *with* $x(t) : [0,+\infty) \mapsto R^n$ *such that*

$$\frac{d}{dt}F(x(t)) \leq aF(x(t)) - bF^{\eta}(x(t)) - cF^{\delta}(x(t)), \ \ x(t) \in R^n \backslash \{\mathbf{0}_n\},$$

where $a \in R$*,* $b, c > 0$ *and* $0 \leq \eta < 1, \delta > 1$*, the following results hold.*

(1) If $a \leq 0$*, there exists* $0 \leq T(x(0)) < +\infty$ *such that* $x(t) = 0$ *for all* $t \geq T(x(0))$ *and*

$$T(x(0)) \leq T_{\max}^1 = \frac{\pi}{(\delta - \eta)b}\Big(\frac{b}{c}\Big)^{\nu}\csc(\nu\pi),$$

where $\nu = \frac{1-\eta}{\delta-\eta}$*.*

(2) If $0 < a < 2\sqrt{bc}$*, and* $\eta + \delta = 2$*, there exists* $0 \leq T(x(0)) < +\infty$ *such that* $x(t) = 0$ *for all* $t \geq T(x(0))$

and

$$T(x(0)) \le T_{\max}^2 = \frac{1}{\delta - 1}\frac{2}{\sqrt{4bc - a^2}}\Big(\frac{\pi}{2} + \arctan(\frac{a}{\sqrt{4bc - a^2}})\Big).$$

Lemma 3 ([33]). *Suppose that* $c_k \ge 0$, $0 < u \le 1$, $v \ge 1$. *Then,*

$$\sum_{k=1}^{s} c_k^u \ge \Big(\sum_{k=1}^{s} c_k\Big)^u, \ \sum_{k=1}^{s} c_k^v \ge s^{1-v}\Big(\sum_{k=1}^{s} c_k\Big)^v.$$

Assumption 1. *There exists a scalar* $\rho > 0$ *such that*

$$\|f(a) - f(b)\| \le \rho\|a - b\|, \ \ a, b \in R^n.$$

3. Main Results

In this section, a quantized boundary controller is devised, and several sufficient criteria are established to ensure the fixed-time synchronization of STCNs (1) by using the Lyapunov method, Wirtinger's inequality, and the technique of integration by parts.

To facilitate subsequent analysis, denote

$$\Sigma = I_m \otimes \Big([\Theta A]^s + \rho\|[\Theta B]^s\|I_n\Big) - \frac{\pi^2}{2L^2}\Pi + \varepsilon[W \otimes \Theta\hat{\Gamma}]^s,$$

$$\Upsilon = I_m \otimes (A + \rho\|B\|I_n - \frac{\pi^2}{4L^2}D) + \varepsilon W \otimes \hat{\Gamma}.$$

To ensure fixed-time synchronization, the boundary controller is designed as

$$U_r(t) = \begin{cases} -\alpha\Psi_r(L,t)V_r^p(t) - \beta\Psi_r(L,t)V_r^q(t), & \sigma_r(L,t) \ne \mathbf{0}_n, \\ \mathbf{0}_n, & \sigma_r(L,t) = \mathbf{0}_n, \end{cases} \tag{4}$$

where $\alpha, \ \beta > 0$ and $0 \le p < 1, \ q > 1, r \in \mathcal{N}$ and

$$\Psi_r(L,t) = \frac{\mathbb{Q}(\sigma_r(L,t))}{\|\mathbb{Q}(\sigma_r(L,t))\|^2}, \ \ V_r(t) = \int_0^L \mathbb{Q}(\sigma_r^T(x,t))\Theta\mathbb{Q}(\sigma_r(x,t))dx,$$

in which $\Theta = \text{diag}\{\Theta_1, \ldots, \Theta_n\} > 0$, $\mathbb{Q}(\sigma_r(x,t)) = (q(\sigma_r^1(x,t)), \ldots, q(\sigma_r^n(x,t)))^T$, $q(v) : R \mapsto \Im$ is the quantizer and satisfies

$$q(v) = \begin{cases} \eta^r\tau_0, & \text{if } \frac{\eta^r\tau_0}{1+\varrho} < v \le \frac{\eta^r\tau_0}{1-\varrho}, \\ 0, & \text{if } \ v = 0, \\ -q(-v), & \text{if } \ v < 0, \end{cases} \tag{5}$$

where $\Im = \{\pm\eta^r\tau_0 | r = 0, \pm1, \pm2, \ldots, \tau_0 > 0\} \cup \{0\}$, $0 < \eta < 1$, $\varrho = \frac{1-\eta}{1+\eta}$ represents the quantification step. It holds that $q(v) - v = \alpha v, \ \alpha \in [-\varrho, \varrho]$, which is considered in [21].

Remark 3. *The controller (4) devised in this paper operates only at boundary* $x = L$. *It has two primary advantages. First, in terms of implementation, unlike the full-domain controllers presented in [36–39], it eliminates the need for extensive deployment of control nodes across the entire spatial domain. Economically, a logarithmic quantization mechanism is incorporated into the boundary controller (4), which effectively reduces the communication burden and computational costs compared to the boundary controller in [29–31,41].*

Theorem 1. *Under Assumption 1 and the quantized boundary controller (4), if there exists a matrix* $\Theta = diag\{\Theta_1, \Theta_2, \ldots, \Theta_n\} > 0$ *such that*

$$\Pi = I_m \otimes \Theta D + \varepsilon W \otimes \Theta\Gamma > 0, \tag{6}$$

then the following results can be derived.

(1) If $\lambda_{\max}(\tilde{\Sigma}) \leq 0$*, the controlled network (1) is fixed-time synchronized and*

$$T^* \leq \bar{T}_1 = \frac{\pi}{\tilde{\alpha}(q-p)}\Big(\frac{\tilde{\alpha}}{\tilde{\beta}}\Big)^{\nu}\csc(\nu\pi),$$

where $\nu = \frac{1-p}{q-p}$, $\tilde{\alpha} = \frac{2\alpha(1-\varrho)^{2p}}{1+\varrho}\lambda_{\min}(\Pi)$, $\tilde{\beta} = \frac{2\beta(1-\varrho)^{2q}}{1+\varrho}m^{1-q}\lambda_{\min}(\Pi)$, $\tilde{\Sigma} = (I_m \otimes M^{-1})^T\Sigma(I_m \otimes M^{-1})$*, in which* M *satisfies* $\Theta = M^TM$.

(2) If $p+q=2$ *and* $0 < \lambda_{\max}(\tilde{\Sigma}) < 2\sqrt{\tilde{\alpha}\tilde{\beta}}$*, the controlled network (1) is fixed-time synchronized and*

$$T^* \leq \bar{T}_2 = \frac{1}{q-1}\frac{2}{\sqrt{4\tilde{\alpha}\tilde{\beta} - \lambda^2_{\max}(\tilde{\Sigma})}}\Big(\frac{\pi}{2} + \arctan\Big(\frac{\lambda_{\max}(\tilde{\Sigma})}{\sqrt{4\tilde{\alpha}\tilde{\beta} - \lambda^2_{\max}(\tilde{\Sigma})}}\Big)\Big).$$

Proof. Construct the following function

$$V(t) = \int_0^L \sigma^T(x,t)(I_m \otimes \Theta)\sigma(x,t)dx.$$

For $\sigma(x,t) \in R^{nm}\backslash\{\mathbf{0}_{nm}\}$,

$$\begin{aligned}\dot{V}(t) = 2\int_0^L \Big[&\sigma^T(x,t)(I_m \otimes \Theta D)\Delta\sigma(x,t)\\ &+ (I_m \otimes \Theta A)\sigma(x,t) + (I_m \otimes \Theta B)F(\sigma(x,t))\Big]dx\\ &+ 2\varepsilon\int_0^L \sigma^T(x,t)(W \otimes \Theta\Gamma)\Delta\sigma(x,t)dx\\ &+ 2\varepsilon\int_0^L \sigma^T(x,t)(W \otimes \Theta\hat{\Gamma})\sigma(x,t)dx. \end{aligned} \tag{7}$$

From Assumption 1,

$$\begin{aligned}&2\int_0^L \sigma^T(x,t)(I_m \otimes \Theta B)F(\sigma(x,t))dx\\ \leq &\int_0^L \sigma^T(x,t)(I_m \otimes \rho\|[\Theta B]^s\|I_n)\sigma(x,t)dx.\end{aligned} \tag{8}$$

Using the technique of integration by parts and the mixed boundary conditions,

$$\begin{aligned}&2\int_0^L \sigma^T(x,t)(I_m \otimes \Theta D)\Delta\sigma(x,t)dx\\ &= 2\sum_{r=1}^m \sigma_r^T(L,t)\Theta D U_r(t) - 2\sum_{r=1}^m \int_0^L \Big(\frac{\partial\sigma_r(x,t)}{\partial x}\Big)^T\Theta D\Big(\frac{\partial\sigma_r(x,t)}{\partial x}\Big)dx\\ &= 2\sigma^T(L,t)(I_m \otimes \Theta D)U(t) - 2\int_0^L \Big(\frac{\partial\sigma(x,t)}{\partial x}\Big)^T(I_m \otimes \Theta D)\Big(\frac{\partial\sigma(x,t)}{\partial x}\Big)dx.\end{aligned} \tag{9}$$

Similarly,

$$\begin{aligned}&2\varepsilon\int_0^L \sigma^T(x,t)(W \otimes \Theta\Gamma)\Delta\sigma(x,t)dx\\ &= 2\varepsilon\sigma^T(L,t)(W \otimes \Theta\Gamma)U(t) - 2\varepsilon\int_0^L \Big(\frac{\partial\sigma(x,t)}{\partial x}\Big)^T(W \otimes \Theta\Gamma)\Big(\frac{\partial\sigma(x,t)}{\partial x}\Big)dx.\end{aligned} \tag{10}$$

Furthermore, from Equations (9) and (10), in light of Lemma 1,

$$\begin{aligned}
&-2\int_0^L \Big(\frac{\partial\sigma(x,t)}{\partial x}\Big)^T (I_m\otimes\Theta D)\Big(\frac{\partial\sigma(x,t)}{\partial x}\Big)dx\\
&-2\varepsilon\int_0^L \Big(\frac{\partial\sigma(x,t)}{\partial x}\Big)^T (W\otimes\Theta\Gamma)\Big(\frac{\partial\sigma(x,t)}{\partial x}\Big)dx\\
&\le -\frac{\pi^2}{2L^2}\int_0^L \sigma^T(x,t)\Pi\sigma(x,t)dx,
\end{aligned} \tag{11}$$

when $\Pi > 0$.

From the quantized boundary controller (4), we have

$$\begin{aligned}
&\sigma^T(L,t)(I_m\otimes\Theta D)U(t)\\
&=-\alpha\sum_{r=1}^m\sum_{k=1}^n \sigma_r^k(L,t)\Theta_k d_k q(\sigma_r^k(L,t))\frac{(V_r(t))^p}{\parallel \mathbb{Q}(\sigma_r(L,t))\parallel^2}\\
&\quad-\beta\sum_{r=1}^m\sum_{k=1}^n \sigma_r^k(L,t)\Theta_k d_k q(\sigma_r^k(L,t))\frac{(V_r(t))^q}{\parallel \mathbb{Q}(\sigma_r(L,t))\parallel^2}\\
&\le -\frac{\alpha(1-\varrho)^{2p}}{1+\varrho}\sum_{k=1}^n(\sigma^k(L,t))^T\Theta_k d_k\tilde{\sigma}^k(L,t)\\
&\quad-\frac{\beta(1-\varrho)^{2q}}{1+\varrho}\sum_{k=1}^n(\sigma^k(L,t))^T\Theta_k d_k\hat{\sigma}^k(L,t),
\end{aligned} \tag{12}$$

and

$$\begin{aligned}
&\varepsilon\sigma^T(L,t)(W\otimes\Theta\Gamma)U(t)\\
&=-\varepsilon\alpha\sum_{r=1}^m\sum_{j=1}^m\sum_{k=1}^n \sigma_r^k(L,t)w_{rj}\Theta_k q(\gamma_k\sigma_j^k(L,t))\frac{(V_j(t))^p}{\parallel \mathbb{Q}(\sigma_j(L,t))\parallel^2}\\
&\quad-\varepsilon\beta\sum_{r=1}^m\sum_{j=1}^m\sum_{k=1}^n \sigma_r^k(L,t)\Theta_k\gamma_k q(\sigma_j^k(L,t))\frac{(V_j(t))^q}{\parallel \mathbb{Q}(\sigma_j(L,t))\parallel^2}\\
&\le -\frac{\varepsilon\alpha(1-\varrho)^{2p}}{1+\varrho}\sum_{k=1}^n(\sigma^k(L,t))^T\Theta_k\gamma_k W\tilde{\sigma}^k(L,t)\\
&\quad-\frac{\varepsilon\beta(1-\varrho)^{2q}}{1+\varrho}\sum_{k=1}^n(\sigma^k(L,t))^T\Theta_k\gamma_k W\hat{\sigma}^k(L,t),
\end{aligned} \tag{13}$$

where

$$\sigma^k(x,t)=(\sigma_1^k(x,t),\sigma_2^k(x,t),\ldots,\sigma_m^k(x,t))^T,$$

$$\tilde{\sigma}^k(x,t)=\Big(\sigma_1^k(x,t)\frac{(V_1(t))^p}{\parallel\sigma_1(L,t)\parallel^2},\sigma_2^k(x,t)\frac{(V_2(t))^p}{\parallel\sigma_2(L,t)\parallel^2},\ldots,\sigma_m^k(x,t)\frac{(V_m(t))^p}{\parallel\sigma_m(L,t)\parallel^2}\Big)^T,$$

$$\tilde{\sigma}^k(x,t)=\Big(\sigma_1^k(x,t)\frac{(V_1(t))^q}{\parallel\sigma_1(L,t)\parallel^2},\sigma_2^k(x,t)\frac{(V_2(t))^q}{\parallel\sigma_2(L,t)\parallel^2},\ldots,\sigma_m^k(x,t)\frac{(V_m(t))^q}{\parallel\sigma_m(L,t)\parallel^2}\Big)^T.$$

From inequalities (12) and (13),

$$\begin{aligned}
&\sigma^T(L,t)\Big[(I_m\otimes\Theta D)+\varepsilon(W\otimes\Theta\Gamma)\Big]U(t)\\
&=-\frac{\alpha(1-\varrho)^{2p}}{1+\varrho}\sum_{k=1}^n\Big(\sigma^k(L,t)\Big)^T(\Theta_k d_k I_m+\varepsilon\Theta_k\gamma_k W)\tilde{\sigma}^k(L,t)\\
&\quad-\frac{\beta(1-\varrho)^{2q}}{1+\varrho}\sum_{k=1}^n\Big(\sigma^k(L,t)\Big)^T(\Theta_k d_k I_m+\varepsilon\Theta_k\gamma_k W)\hat{\sigma}^k(L,t)\\
&\le -\frac{\alpha(1-\varrho)^{2p}}{1+\varrho}\lambda_{\min}(\Pi)\sum_{r=1}^m(V_r(t))^p-\frac{\beta(1-\varrho)^{2q}}{1+\varrho}\lambda_{\min}(\Pi)\sum_{r=1}^m(V_r(t))^q.
\end{aligned} \tag{14}$$

Considering Lemma 3, for $0 \leq p < 1$,

$$\sum_{r=1}^{m}\Big(V_r(t)\Big)^p \geq \Big(\sum_{r=1}^{m}V_r(t)\Big)^p,$$

and for $q > 1$,

$$\sum_{r=1}^{m}\Big(V_r(t)\Big)^q \geq m^{1-q}\Big(\sum_{r=1}^{m}V_r(t)\Big)^q,$$

submit them into the inequality (14),

$$\begin{aligned}&\sigma^T(L,t)\Big[(I_m\otimes\Theta D)+\varepsilon(W\otimes\Theta\Gamma)\Big]U(t)\\ &\leq -\frac{\alpha(1-\varrho)^{2p}}{1+\varrho}\lambda_{\min}(\Pi)V^p(t)-\frac{\beta(1-\varrho)^{2q}}{1+\varrho}\lambda_{\min}(\Pi)m^{1-q}V^q(t).\end{aligned}\tag{15}$$

Substituting (8)–(15) into equation (7), for $\sigma(x,t)\in R^{nm}\backslash\{\mathbf{0}_{nm}\}$,

$$\begin{aligned}\dot{V}(t)\leq&\int_0^L\sigma^T(x,t)\Big[I_m\otimes\Big([\Theta A]^s+\rho\|[\Theta B]^s\|I_n\Big)\Big]\sigma(x,t)dx\\ &-\frac{\pi^2}{2L^2}\int_0^L\sigma^T(x,t)\Pi\sigma(x,t)dx+\varepsilon\int_0^L\sigma^T(x,t)[W\otimes\Theta\hat{\Gamma}]^s\sigma(x,t)dx\\ &-\frac{2\alpha(1-\varrho)^{2p}}{1+\varrho}\lambda_{\min}(\Pi)V^p(t)-\frac{2\beta(1-\varrho)^{2q}}{1+\varrho}\lambda_{\min}(\Pi)m^{1-q}V^q(t)\\ =&\int_0^L\sigma^T(x,t)\Sigma\sigma(x,t)dx-\tilde{\alpha}V^p(t)-\tilde{\beta}V^q(t).\end{aligned}$$

Additionally, according to the matrix decomposition theory, there exists a real invertible matrix M such that $\Theta = M^TM$, then

$$\begin{aligned}&\int_0^L\sigma^T(x,t)\Sigma\sigma(x,t)dx\\ =&\int_0^L\Big((I_m\otimes M)\sigma(x,t)\Big)^T(I_m\otimes M^{-1})^T\Sigma(I_m\otimes M^{-1})\Big((I_m\otimes M)\sigma(x,t)\Big)dx\\ \leq&\lambda_{\max}(\tilde{\Sigma})\int_0^L\Big((I_m\otimes M)\sigma(x,t)\Big)^T\Big((I_m\otimes M)\sigma(x,t)\Big)dx.\end{aligned}$$

Thus, we have

$$\dot{V}(t)\leq\lambda_{\max}(\tilde{\Sigma})V(t)-\tilde{\alpha}V^p(t)-\tilde{\beta}V^q(t).$$

If $\lambda_{\max}(\tilde{\Sigma})\leq 0$, all $\sigma(x,t)\in R^{nm}\backslash\{\mathbf{0}_{nm}\}$ correspond to case (1) in Lemma 3. In this case, the fixed-time synchronization of the network (1) is guaranteed within the time $\bar{T}_1$.

Similarly, if $p+q=2$ and $0<\lambda_{\max}(\tilde{\Sigma})<2\sqrt{\tilde{\alpha}\tilde{\beta}}$, this corresponds to case (2) in Lemma 3. Then, the network (1) is synchronized within the time $\bar{T}_2$. □

Remark 4. *It is noteworthy that most existing studies on the boundary synchronization of STCNs have focused exclusively on Neumann boundary conditions[15–19,29]. Nonetheless, Lemma 1 cannot be directly applied under Neumann boundary conditions, and these studies necessitate complex variable transformations in their theoretical analyses. In contrast, Theorem 1 of this article utilizes mixed boundary conditions, which not only eliminates the need for variable transformation but also simplifies the analytical procedure. In addition, the synchronization criteria derived here are easier to verify than those presented in previous works [15–19,29].*

Next, consider a special case for STCNs (1) without spatial diffusion coupling, i.e., $\varepsilon\sum_{j=1}^{m}w_{rj}\Gamma\Delta z_j(x,t)=0$. *Here, the mixed boundary conditions corresponding to system (1) with state coupling are redefined as*

$$z_r(0,t)=\mathbf{0}_n,\quad\frac{\partial z_r(x,t)}{\partial x}\Big|_{x=L}=\hat{U}_r(t),$$

where $t \in [0, +\infty)$, $\hat{U}_r(t) = (\hat{U}_r^1(t), \hat{U}_r^2(t), \ldots, \hat{U}_r^n(t))^T$ *is designed by*

$$\hat{U}_r(t) = \begin{cases} -\alpha\hat{\Psi}_r(L,t)\hat{V}_r^{\hat{p}}(t) - \beta\hat{\Psi}_r(L,t)\hat{V}_r^{\hat{q}}(t), & \sigma_r(L,t) \neq \mathbf{0}_n, \\ \mathbf{0}_n, & \sigma_r(L,t) = \mathbf{0}_n, \end{cases} \tag{16}$$

where $\alpha,\ \beta > 0$ *and* $0 \leq \hat{p} < 1,\ \hat{q} > 1$, *and*

$$\hat{V}_r(t) = \int_0^L q^T(\sigma_r(x,t))q(\sigma_r(x,t))dx,$$

$$\hat{\Psi}_r(L,t) = \Big(\frac{sign(q(\sigma_r^1(L,t)))}{\mid q(\sigma_r^1(L,t)) \mid}, \frac{sign(q(\sigma_r^2(L,t)))}{\mid q(\sigma_r^2(L,t) \mid}, \ldots, \frac{sign(q(\sigma_r^n(L,t)))}{\mid q(\sigma_r^n(L,t))) \mid}\Big)^T.$$

Theorem 2. *Under Assumption 1 and the quantized boundary controller (16), the following results can be derived.*

(1) If $\lambda_{\max}(\Upsilon) \leq 0$, *the controlled network (1) without spatial diffusion coupling is fixed-time synchronized and*

$$T^* \leq \hat{T}_1 = \frac{\pi}{\hat{\alpha}(\hat{q}-\hat{p})}\Big(\frac{\hat{\alpha}}{\hat{\beta}}\Big)^{\nu}\csc(\nu\pi),$$

where $\nu = \frac{1-\hat{p}}{\hat{q}-\hat{p}}$, $\hat{\alpha} = \lambda_{\min}(D)\frac{\alpha(1-\varrho)^{2\hat{p}}}{1+\varrho}$, $\hat{\beta} = m^{1-\hat{q}}\lambda_{\min}(D)\frac{\beta(1-\varrho)^{2\hat{q}}}{1+\varrho}$.

(2) If $\hat{p}+\hat{q} = 2$ *and* $0 < \lambda_{\max}(\Upsilon) < 2\sqrt{\hat{\alpha}\hat{\beta}}$, *the controlled network (1) without spatial diffusion coupling is fixed-time synchronized and*

$$T^* \leq \hat{T}_2 = \frac{1}{\hat{q}-1}\frac{2}{\sqrt{4\hat{\alpha}\hat{\beta} - \lambda_{\max}^2(\Upsilon)}}\Big(\frac{\pi}{2} + \arctan\Big(\frac{\lambda_{\max}(\Upsilon)}{\sqrt{4\hat{\alpha}\hat{\beta} - \lambda_{\max}^2(\Upsilon)}}\Big)\Big).$$

Proof. Construct the following function

$$\hat{V}(t) = \frac{1}{2}\int_0^L \sigma^T(x,t)\sigma(x,t)dx.$$

For $\sigma(x,t) \in R^{nm}\backslash\{\mathbf{0}_{nm}\}$ and $\varepsilon\sum_{j=1}^{m} w_{rj}\Gamma\Delta z_j(x,t) = 0$,

$$\begin{aligned}\dot{\hat{V}}(t) = &\sum_{r=1}^{m}\int_0^L \sigma_r^T(x,t)\Big[D\Delta\sigma_r(x,t) + A\sigma_r(x,t) + B\tilde{f}(\sigma_r(x,t))\Big]dx \\ &+ \varepsilon\sum_{r=1}^{m}\sum_{j=1}^{m}\int_0^L \sigma_r^T(x,t)w_{rj}\hat{\Gamma}\sigma_j(x,t)dx.\end{aligned} \tag{17}$$

Using the technique of integration by parts and the mixed boundary conditions,

$$\begin{aligned}&\sum_{r=1}^{m}\int_0^L \sigma_r^T(x,t)D\Delta\sigma_r(x,t)dx \\ &= \sigma^T(L,t)(I_m\otimes D)\hat{U}(t) - \int_0^L \Big(\frac{\partial\sigma(x,t)}{\partial x}\Big)^T(I_m\otimes D)\Big(\frac{\partial\sigma(x,t)}{\partial x}\Big)dx,\end{aligned} \tag{18}$$

where $\hat{U}(t) = (\hat{U}_1^T(t), \hat{U}_2^T(t), \ldots, \hat{U}_m^T(t))^T$.

By utilizing Lemma 1,

$$\begin{aligned}&-\int_0^L \Big(\frac{\partial\sigma(x,t)}{\partial x}\Big)^T(I_m\otimes D)\Big(\frac{\partial\sigma(x,t)}{\partial x}\Big)dx \\ &\leq -\frac{\pi^2}{4L^2}\int_0^L \sigma^T(x,t)(I_m\otimes D)\sigma(x,t)dx.\end{aligned} \tag{19}$$

Using the boundary controller (16), Lemma 3, and $\text{sign}(q(\sigma_r^k(\nu,t))) = \text{sign}(\sigma_r^k(\nu,t))$, we have

$$\begin{aligned}
&\sigma^T(L,t)(I_m \otimes D)\hat{U}(t)\\
&= -\hat{\alpha}\sum_{r=1}^{m}\sum_{k=1}^{n}\frac{\sigma_r^k(L,t)d_k\text{sign}(q(\sigma_r^k(L,t)))}{\mid q(\sigma_r^k(L,t))\mid}(\hat{V}_r(t))^{\hat{p}}\\
&\quad -\hat{\beta}\sum_{r=1}^{m}\sum_{k=1}^{n}\frac{\sigma_r^k(L,t)d_k\text{sign}(q(\sigma_r^k(L,t)))}{\mid q(\sigma_r^k(L,t))\mid}(\hat{V}_r(t))^{\hat{q}}\\
&\le -\lambda_{\min}(D)\frac{\alpha(1-\varrho)^{2\hat{p}}}{1+\varrho}(\sum_{r=1}^{m}\hat{V}_r(t))^{\hat{p}} - \lambda_{\min}(D)m^{1-\hat{q}}\frac{\beta(1-\varrho)^{2\hat{q}}}{1+\varrho}(\sum_{r=1}^{m}\hat{V}_r(t))^{\hat{q}}.
\end{aligned} \tag{20}$$

Substituting (18)–(20) into equation (17), one has

$$\begin{aligned}
\dot{\hat{V}}(t) &\le \int_0^L \sigma^T(x,t)\Big[I_m \otimes (A+\rho\|B\|I_n) + \varepsilon W \otimes \hat{\Gamma}\Big]\sigma(x,t)dx\\
&\quad -\frac{\pi^2}{4L^2}\int_0^L \sigma^T(x,t)(I_m\otimes D)\sigma(x,t)dx\\
&\quad -\frac{\alpha(1-\varrho)^{2\hat{p}}}{1+\varrho}\lambda_{\min}(D)V^{\hat{p}}(t) - m^{1-\hat{q}}\frac{\beta(1-\varrho)^{2\hat{q}}}{1+\varrho}\lambda_{\min}(D)V^{\hat{q}}(t)\\
&= \int_0^L \sigma^T(x,t)\Upsilon\sigma(x,t)dx - \hat{\alpha}\hat{V}^{\hat{p}}(t) - \hat{\beta}\hat{V}^{\hat{q}}(t)\\
&\le \lambda_{\max}(\Upsilon)\hat{V}(t) - \hat{\alpha}\hat{V}^{\hat{p}}(t) - \hat{\beta}\hat{V}^{\hat{q}}(t),
\end{aligned}$$

for $\sigma(x,t) \in R^{nm}\backslash\{\mathbf{0}_{nm}\}$.

If $\lambda_{\max}(\Upsilon) \le 0$, all $\sigma(x,t) \in R^{nm}\backslash\{\mathbf{0}_{nm}\}$ correspond to case (1) in Lemma 3. In this case, the network (1) is synchronized within the time $\hat{T}_1$.

Similarly, if $\hat{p}+\hat{q} = 2$ and $0 < \lambda_{\max}(\Upsilon) < 2\sqrt{\hat{\alpha}\hat{\beta}}$, this corresponds to case (2) in Lemma 3. Then, the fixed-time synchronization of network (1) is guaranteed within the time $\hat{T}_2$. □

Remark 5. *In [30,31,41], the limited-time boundary synchronization of STCNs with mixed boundary conditions was investigated using the Lyapunov method. Notably, the boundary controllers proposed by them comprise a linear feedback term* $-k\sigma_r(L,t)$ *or* $\int_0^L k\sigma_r(x,t)$ *with* $k > 0$ *and two power-law terms* $\frac{-k_1\sigma_r(L,t)\|(\sigma_r(x,t))\|_{\mathcal{L}_2}^{\delta}}{\|(\sigma_r(L,t))\|^2}$ *(*$k_1 > 0, 0 < \delta < 1$*) and* $\frac{-k_2\sigma_r(L,t)\|(\sigma_r(x,t))\|_{\mathcal{L}_2}^{\theta}}{\|(\sigma_r(L,t))\|^2}$ *(*$k_2 > 0, \theta > 1$*). Consequently, the differential inequality* $\dot{V}(t) \le \phi V(t) - \phi_1 V^p(t) - \phi_2 V^q(t)$ *was derived, where* $\phi < 0$ *is a necessary condition for achieving synchronization. However, the condition* $\phi < 0$ *may be restrictive in practical applications. Moreover, recent studies in [33,35] have demonstrated that fixed-time synchronization can also be achieved using the controllers comprised of pure power-law forms. Inspired by this,* ϕ *is set to an arbitrary constant, and the pure power-law boundary controllers (4) and (16) without linear feedback are designed in this paper. In the analysis of Theorems 1 and 2, these power-law terms yield two key terms* $-\tilde{\alpha}V^p(t)$ *and* $-\tilde{\beta}V^q(t)$ *(*$-\hat{\alpha}\hat{V}^{\hat{p}}(t)$ *and* $-\hat{\beta}\hat{V}^{\hat{q}}(t)$*), which determine the convergence at a fixed time.*

Remark 6. *It should be noted that limited-time quantized synchronization problems have been explored in [23,24,35]. Nonetheless, the dynamic evolution of their concerned system depends only on temporal variables, rather than being co-determined by both time and space. Furthermore, although [20,42] addressed asymptotic or fixed-time synchronization of STCNs through quantized boundary control, these studies primarily focused on state coupling while neglecting the essential role of spatial diffusion coupling. Consequently, the issue and the system examined in this paper are more general.*

4. Numerical Simulations

In this section, two numerical examples are presented to demonstrate the effectiveness of the fixed-time synchronization results.

Example 1. *Consider a three-dimensional spatiotemporal system*

$$\frac{\partial \xi(x,t)}{\partial t} = D\frac{\partial^2 \xi(x,t)}{\partial x^2} - A\xi(x,t) + Bf(\xi(x,t)), \tag{21}$$

and a spatiotemporal network with 50 *nodes whose dynamic is described as*

$$\begin{aligned}\frac{\partial z_r(x,t)}{\partial t} =& D\Delta z_r(x,t) - Az_r(x,t) + Bf(z_r(x,t)) \\ &+ \varepsilon \sum_{j=1}^{50} w_{rj}\Gamma \Delta z_j(x,t) + \varepsilon \sum_{j=1}^{50} w_{rj}\hat{\Gamma} z_j(x,t), \quad r = 1,2,\ldots,50,\end{aligned} \tag{22}$$

where $z_r(x,t) = (z_r^1(x,t), z_r^2(x,t), z_r^3(x,t))^T$, $(x,t) \in [-1,1] \times [0,+\infty)$. *The corresponding parameters are listed in Table 1.*

Table 1. Parameters.

System Parameters
$\varepsilon = 0.02$, $A = I_3$, $D = 0.5I_3$, $\Gamma = \hat{\Gamma} = I_3$, $f(\xi) = (\tanh(\xi^1), \tanh(\xi^2), \tanh(\xi^3))^T$, $B = \begin{bmatrix} 2 & -1.2 & 3.5 \\ 2.0 & 2.71 & 3.9 \\ -4.8 & -1.5 & 1.1 \end{bmatrix}$, W generated by the NW algorithm where all edge weights are equal to 1.
The Initial and Boundary Conditions
$\xi(-1,t) = \frac{\partial \xi(x,t)}{\partial x}\big\|_{x=1} = \mathbf{0}_3$, $z_r(-1,t) = \mathbf{0}_3$, $\frac{\partial z_r(x,t)}{\partial x}\big\|_{x=1} = U_r(t)$, $\xi(x,0) = (\xi^1(x,0), \xi^2(x,0), \xi^3(x,0))^T = (0.01, 0.05, 0.1)^T$, $z_r(x,0) = (z_r^1(x,0), z_r^2(x,0), z_r^3(x,0))^T$ are randomly determined in $[-5,5]$.
Control Parameters in Theorem 1
Control parameters: $\alpha = 20$, $\beta = 25$, $p = 0.95$, $q = 1.05$. Quantization parameters: $\eta = 0.8$ $\tau_0 = 30$.
Control Parameters in Theorem 2
Control parameters: $\alpha = 18$, $\beta = 12$, $\hat{p} = 0.9$, $\hat{q} = 1.1$. Quantization parameters: $\eta = 0.5$ $\tau_0 = 30$.

The topology of the system (22) is represented as an undirected graph randomly generated by the NW algorithm, where all edge weights are equal to 1, as illustrated in Figure 1. In the absence of quantized boundary control, the trajectories of $\sigma_r(x,t) = z_r(x,t) - \xi(x,t)$ are demonstrated in Figure 2. In the following, the fixed-time synchronization of system (22) is established under the boundary controller (4). By selecting the control parameters listed in Table 1, it is straightforward to verify that $\Pi > 0$ when $\Theta = I_3$. Through simple calculation, we have $\lambda_{\min}(\Pi) = 0.2658$, $\lambda_{\max}(\tilde{\Sigma}) = 5.2585 < 2\sqrt{\tilde{\alpha}\tilde{\beta}} = 13.6888$. According to Theorem 1, the network (22) is fixed-time synchronized within $\bar{T}_2 = 6.2194$. The synchronization trajectories of $\sigma_r(x,t) = z_r(x,t) - \xi(x,t)$ are depicted in Figure 3.

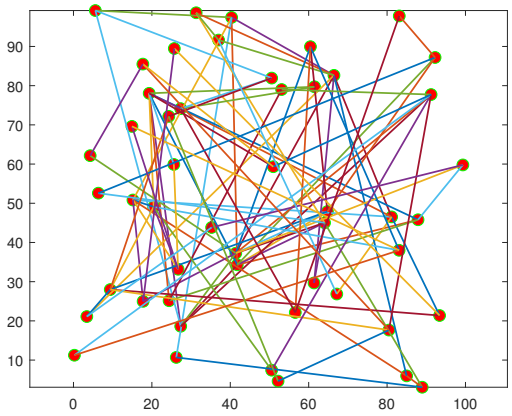

Figure 1. Topology structure of the network (22).

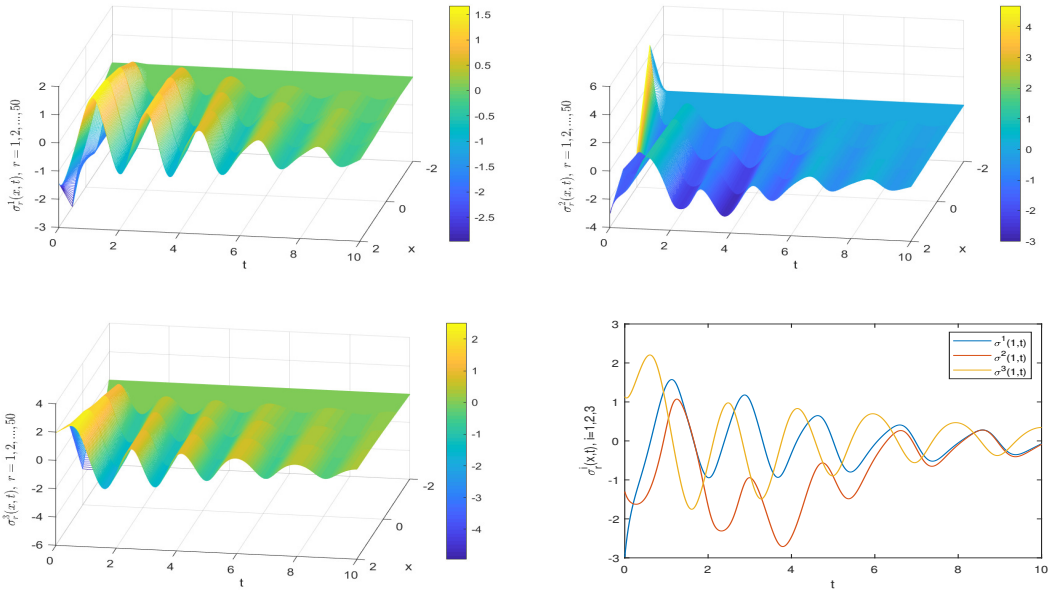

Figure 2. The evolution of the error $\sigma_r^i(x,t)$ and $q(\sigma_r^i(x,t))$ without control.

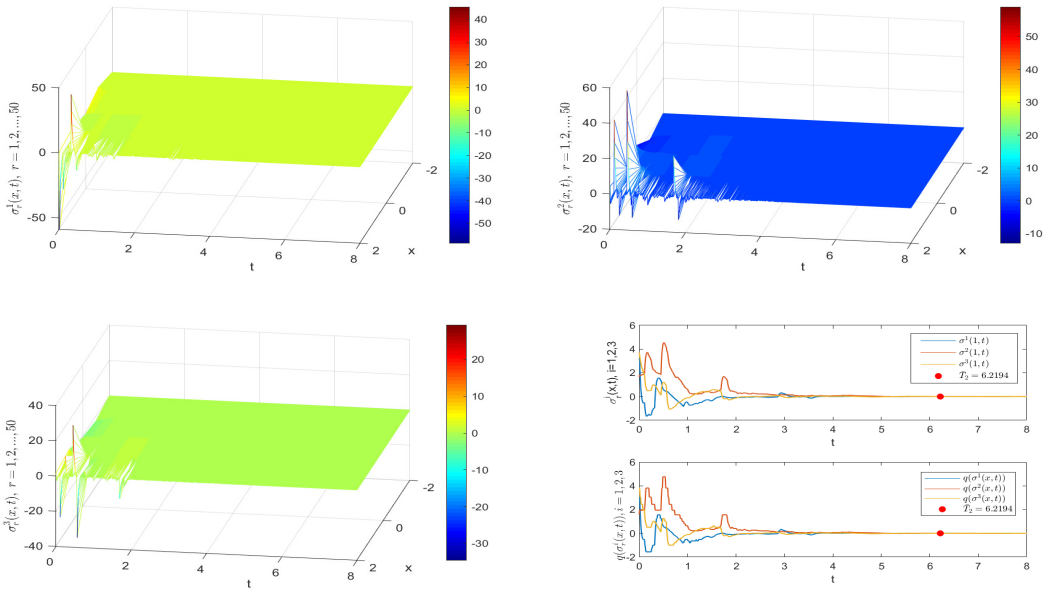

Figure 3. Synchronization evolution under quantized boundary controller (4).

Example 2. *Consider the spatial diffusion coupling* $\varepsilon \sum_{j=1}^{m} w_{rj}\Gamma\Delta z_j(x,t) = 0$ *in system (22). The dynamical evolution of synchronization error without control is demonstrated in Figure 4. To verify fixed-time synchronization of the STCN (22) with state coupling under quantized boundary controller (16), the control parameters listed in Table 1 are selected. It is straightforward to calculate that* $\lambda_{\max}(\Upsilon) = 5.2585 < 2\sqrt{\hat{\alpha}\hat{\beta}} = 8.0573$. *According to Theorem 2, the STCN (22) with state coupling is fixed-time synchronized within* $\hat{T}_2 = 7.4757$. *The simulation results are presented in Figure 5.*

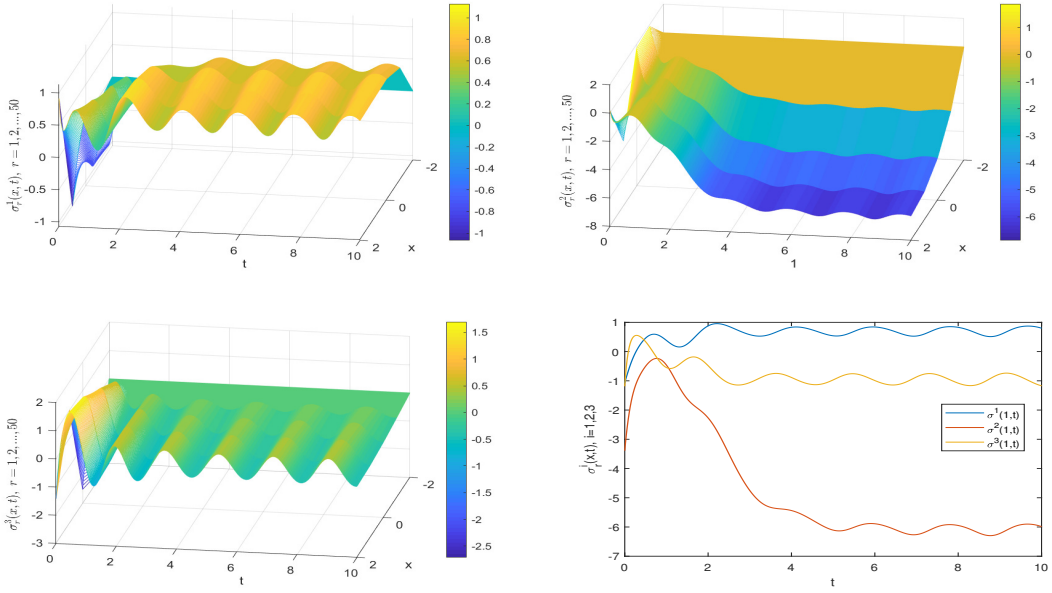

Figure 4. The evolution of the synchronization error $\sigma_r^i(x,t)$ without control.

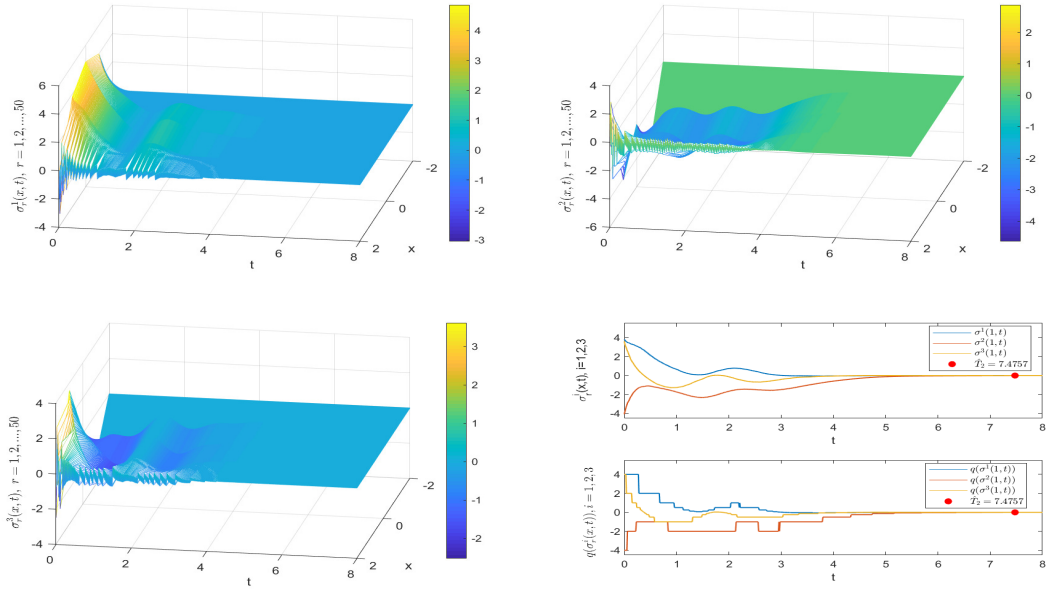

Figure 5. Synchronization evolution under quantized boundary controller (16).

Remark 7. *This article presents two numerical examples to verify the effectiveness of Theorems 1 and 2. First, the dynamical evolution of synchronization error without control is illustrated in Figures 2 and 4. As shown in the figures, the STCN (22) with and without spatial diffusion coupling fails to achieve fixed-time synchronization without control. Meanwhile, the dynamical evolution of synchronization error under the boundary controllers (4) and (16) is demonstrated in Figures 3 and 5, respectively. It can be seen from the figures that the error states converge to zero within the estimated time* $\bar{T}_2 = 6.2194$ *and* $\hat{T}_2 = 7.4757$.

5. Conclusions

This article investigated the fixed-time synchronization of coupled STCNs with mixed boundary conditions through quantized boundary control. For the STCNs with or without spatial diffusion coupling, two effective quantized boundary controllers with pure power-law forms were devised, which are more economical and easier to implement than the full-domain controller presented in [7,8,10]. Utilizing these control schemes and the fixed-time stability theorem, several synchronization criteria were derived for STCNs with or without spatial diffusion coupling, which are more flexible and easier to verify compared to those proposed in [30,31].

It should be noted that the numerical simulation in this paper relies on idealized models (such as perfect actuators and noise-free measurements). Real-world disturbances (e.g., sensor noise, uncertain parameters, actuator delays, and faults) may not be adequately represented. Additionally, recent advancements in quantized fixed-time synchronization have been extensively applied in image encryption and the thermal propagation control of semiconductor power chips [35,43], providing a framework for the practical application of the theoretical results presented in this article. Meanwhile, the boundary prescribed-time stabilization for STCNs has begun to emerge as an active research field [44]. These developments motivate us to explore robust prescribed-time boundary synchronization and its applications in STCNs subject to disturbances in our future work.

Author Contributions

T.S. methodology, writing—original draft, software. C.H. methodology, software, writing-reviewing and editing, funding acquisition. J.Y. supervision, formal analysis, funding acquisition. All authors have read and agreed to the published version of the manuscript.

Funding

This work was supported by National Natural Science Foundation of China (Grant No. 62373317), by the Key Project of Natural Science Foundation of Xinjiang (2021D01D10), by Tianshan Talent Training Program (2022TSYCCX0013) and Intelligent Control and Optimization Research Platform in Xinjiang University.

Conflicts of Interest

The authors declare no conflict of interest.

References

1. Dubey, B.; Das, B.; Hussain, J. A predator-prey interaction model with self and cross-diffusion. *Ecol. Model* **2001**, *141*, 67–76.
2. Roussel, C.; Roussel, M. Reaction-diffusion models of development with state-dependent chemical diffusion coefficients. *Prog. Biophys. Mol. Biol.* **2004**, *86*, 113–160.
3. Chua, L.; Roska, T. The CNN paradigm. *IEEE Trans. Circuits Syst. Fundam. Theory Appl.* **1993**, *40*, 147–156.
4. Wang, L.; Zhang, C. Exponential synchronization of memristor-based competitive neural networks with reaction-diffusions and infinite distributed delays. *IEEE Trans. Neural Netw. Learn. Syst.* **2024**, *35*, 745–758.
5. Baccoli, A.; Pisano, A.; Orlov, Y. Boundary control of coupled reaction-diffusion processes with constant parameters. *Automatica* **2015**, *54*, 80–90.
6. Liu, X.; Wu, K.; Zhang, W. Intermittent boundary stabilization of stochastic reaction-diffusion Cohen-Grossberg neural networks. *Neural Netw.* **2020**, *131*, 1–13.
7. Lin, J.; Xu, R.; Li, L. Spatio-temporal synchronization of reaction-diffusion BAM neural networks via impulsive pinning control. *Neurocomputing* **2020**, *418*, 300–313.
8. Wu, T.; Cao, J.; Xiong, L.; et al. Adaptive event-triggered mechanism to synchronization of reaction-diffusion CVNNs and its application in image secure communication. *IEEE Trans. Syst. Man, Cybern. Syst.* **2023**, *53*, 5307–5320.
9. Khan, A.; Javeed, M.; Hassan, W.; et al. Event-triggered consensus control with dynamic agents and communication delays in heterogeneous multi-agent systems. *Alex. Eng. J.* **2025**, *128*, 1–11.
10. Song, X.; Wang, M.; Song, S.; et al. Intermittent pinning synchronization of reaction-diffusion neural networks with multiple spatial diffusion couplings. *Neural Comput. Appl.* **2019**, *31*, 9279–9294.
11. An, X.; Zhang, L.; Li, Y.; et al. Synchronization analysis of complex networks with multi-weights and its application in public traffic network. *Phys. A Stat. Mech. Appl.* **2014**, *412*, 149–156.
12. Halleux, J.; Prieur, C.; Coron, J.; et al. Boundary feedback control in networks of open channels. *Automatica* **2003**, *39*, 1365–1376.
13. Tang, L.; Zhang, X.; Liu, Y. Boundary controller design for flexible riser systems with input quantization and position constraint. *Automatica* **2024**, *168*, 111815.

14. Wu, K.; Tian, T.; Wang, L. Synchronization for a class of coupled linear partial differential systems via boundary control. *J. Frankl. Inst.* **2016**, *353*, 4026–4073.
15. Liu, X.; Wu, K.; Li, Z. Exponential stabilization of reaction-diffusion systems via intermittent boundary control. *IEEE Trans. Autom. Control* **2022**, *67*, 3036–3042.
16. Wu, K.; Tian, T.; Wang, L.; et al. Asymptotical synchronization for a class of coupled time-delay partial differential systems via boundary control. *Neurocomputing* **2016**, *197*, 113–118.
17. Yang, C.; Cao, J.; Huang, T.; et al. Guaranteed cost boundary control for cluster synchronization of complex spatio-temporal dynamical networks with community structure. *Sci. China Inf. Sci.* **2018**, *61*, 052203.
18. Yang, C.; Huang, T.; Li, Z.; et al. Synchronization of nonlinear complex spatio-temporal networks using adaptive boundary control and pinning adaptive boundary control. *IEEE Access* **2018**, *6*, 38216–38224.
19. He, H. Asymptotical synchronization of coupled time-delay partial differential systems via pinning control and boundary control. *Int. J. Adv. Netw. Appl.* **2020**, *11*, 4443–4450.
20. Liu, F.; Yang, Y.; Wang, F.; et al. Synchronization of fractional-order reaction-diffusion neural networks with Markov parameter jumping: Asynchronous boundary quantization control. *Chaos, Solitons Fractals* **2023**, *173*, 113622.
21. Yang, X.S.; Cheng, Z.H.; Li, X.; et al. Exponential synchronization of coupled neutral-type neural networks with mixed delays via quantized output control. *J. Frankl. Inst.* **2019**, *356*, 8138–8153.
22. Meng, P.; Kong, F.; Zhu, Q.; et al. Quantized control based on fixed-time and predefined-time stabilization of coupled Filippov systems on networks with mismatched parameters. *Nonlinear Dyn.* **2025**, *113*, 10043–10060.
23. Xiong, X.; Yang, X.; Cao, J.; et al. Finite-time control for a class of hybrid systems via quantized intermittent control. *Sci. China Inf. Sci.* **2020**, *63*, 192201.
24. Yang, X.; Cao, J.; Xu, C.; et al. Finite-time stabilization of switched dynamical networks with quantized couplings via quantized controller. *Sci. China Technol. Sci.* **2018**, *61*, 299–308.
25. Wu, K.; Chen, B. Synchronization of partial differential systems via diffusion coupling. *IEEE Trans. Circuits Syst. I Regul. Pap.* **2012**, *59*, 2655–2668.
26. Bhat, S.; Bernstein, D. Finite-time stability of continuous autonomous systems. *SIAM J. Control Optim.* **2000**, *38*, 751–766.
27. Xu, Y.; Liu, W.; Wu, Y.; et al. Finite-time synchronization of fractional-order fuzzy time-varying coupled neural networks subject to reaction-diffusion. *IEEE Trans. Fuzzy Syst.* **2023**, *31*, 3423–3432.
28. Franceschelli, M.; Pisano, A.; Giua, A.; et al. Finite-time consensus with disturbance rejection by discontinuous local interactions in directed graphs. *IEEE Trans. Autom. Control* **2015**, *60*, 1133–1138.
29. Luo, Y.; Ling, Z.; Yao, Y. Finite time synchronization for reactive diffusion complex networks via boundary control. *IEEE Access* **2019**, *7*, 68628–68635.
30. Wu, K.; Sun, H.; Shi, P.; et al. Finite-time boundary stabilization of reaction-diffusion systems. *Int. J. Robust Nonlinear Control* **2018**, *28*, 1641–1652.
31. Wu, K.; Sun, H.; Shi, P.; et al. Finite-time boundary control for delay reaction-diffusion systems. *Appl. Math. Comput.* **2018**, *329*, 52–63.
32. Polyakov, A. Nonlinear feedback design for fixed-time stabilization of linear control systems. *IEEE Trans. Autom. Control* **2012**, *57*, 2106–2110.
33. Hu, C.; Jiang, H. Special functions-based fixed-time estimation and stabilization for dynamic systems. *IEEE Trans. Syst. Man Cybern. Syst.* **2022**, *52*, 3251–3262.
34. Hu, C.; He, H.; Jiang, H. Fixed/Preassigned-time synchronization of complex networks via improving fixed-time stability. *IEEE Trans. Cybern.* **2020**, *51*, 2882–2892.
35. Gao, Y.; Yu, J.; Hu, C.; et al. Fixed/preassigned-time output synchronization for T-S fuzzy complex networks via quantized control. *Nonlinear Anal. Hybrid Syst.* **2024**, *51*, 101434.
36. Wang, Z.; Cao, J.; Cai, Z.; et al. Anti-Synchronization in Fixed time for discontinuous reaction-diffusion neural networks with time-varying coefficients and time delay. *IEEE Trans. Cybern.* **2019**, *50*, 2758–2769.
37. Lian, D.; Min, S. Synchronization in finite-/fixed-time of delayed diffusive complex-valued neural networks with discontinuous activations. *Chaos Solitons Fractals* **2021**, *142*, 110386.
38. Duan, L.; Shi, M.; Huang, L. New results on finite-/fixed-time synchronization of delayed diffusive fuzzy HNNs with discontinuous activations. *Fuzzy Sets Syst.* **2021**, *416*, 141–151.
39. Song, X.; Man, J.; Song, S.; et al. Finite/fixed-time synchronization for Markovian complex-valued memristive neural networks with reaction-diffusion terms and its application. *Neurocomputing* **2020**, *414*, 131–142.
40. Espitia, N.; Polyakov, A.; Efimov, D.; et al. Boundary time-varying feedbacks for fixed-time stabilization of constant-parameter reaction-diffusion systems. *Automatica* **2019**, *103*, 398–407.
41. Li, Z.; Liu, X.; Wu, K.; et al. Fixed-time boundary stabilisation for delay reaction-diffusion systems. *Int. J. Control* **2024**, *97*, 272–283.
42. Shi, T.; Hu, C.; Yu, J.; et al. Fixed-time quantized synchronization of spatiotemporal networks with output-based quantization communication via boundary control. *J. Frankl. Inst.* **2025**, *362*, 107460.

43. Peng, Z.; Song, X.; Song, S.; et al. Hysteresis quantified control for switched reaction-diffusion systems and its application. *Complex Intell. Syst.* **2023**, *9*, 7451–7460.
44. Zekraoui, S.; Espitia, N.; Perruquetti, W. Output-feedback stabilization in prescribed-time of a class of reaction-diffusion PDEs with boundary input delay. *IEEE Trans. Autom. Control* **2025**, *70*, 5066–5081. https://doi.org/10.1109/TAC.2025.3535189.